Thermodynamic bounds from Otto–Villani functional inequalities

Andrea Auconi *
Ca' Foscari University of Venice, DSMN–via Torino 155, 30172 Mestre (Venice), Italy

(Received 15 June 2026; revised 3 October 2026; accepted 27 October 2026; published 12 November 2026)

The dissipation in the relaxation of an ensemble of conservative stochastic systems toward the equilibrium steady state is quantified by the free-energy difference. Functional inequalities within the framework of Otto and Villani [J. Funct. Anal. **173**, 361 (2000)] are here revisited which connect the free-energy dynamics and optimal transport, offering a geometric perspective on the instantaneous speed of relaxation in the presence of potential barriers. These are illustrated with numerical relaxation experiments on Landau-Ginzburg potentials. The same inequalities hold for relaxation toward nonequilibrium steady states once the potential is replaced by the pseudopotential defined by the stationary density.

DOI: 10.1103/6zkl-1vnk

I. INTRODUCTION

In nonequilibrium thermodynamics [1–3], a system's response to sudden changes in external conditions fundamentally manifests as transient relaxation dynamics. These relaxation processes are found across various fields, ranging from sensory adaptation in biophysics [4–6] and bit erasure in information processing [7–10] to Mpemba effects in thermal phenomena [11–15].

For continuous systems, relaxation processes are typically described at the ensemble level in terms of the Fokker-Planck equation [16–18], and the time derivative of the relative entropy from the steady state is a measure of instantaneous relaxation speed. This has the mathematical form of a relative Fisher information [19] and the thermodynamic interpretation of an excess entropy production rate [20–24].

Thermodynamic speed limits formalize the trade-off between the entropy production in a finite-time process and its duration [25,26]. In this framework, the Benamou-Brenier formulation of optimal transport [27] has been considered as a variational principle to derive speed limits in terms of the Wasserstein distance [28–34]. These speed limits are inherently defined for finite-time processes, as indeed when applied to bound the instantaneous relaxation speed they either reduce to the definition of the entropy production rate or simply vanish.

The Otto–Villani HWI inequality [35–38] offers a lower bound on the instantaneous relaxation speed based on the Wasserstein distance and the minimum convexity of the potential. Although the HWI bound is tighter than the logarithmic Sobolev inequality (LSI), this worst-case scenario on the potential landscape makes it typically loose in nonconvex potentials. In contrast, this paper highlights an intermediate bound in the HWI derivation that provides the fundamental connection between physical density dynamics and optimal transport and offers a geometric perspective on thermal relaxation. After reviewing the functional inequalities with optimal transport, the predictive power of the various bounds is illustrated analytically on a 1D Gaussian expansion and numerically on a double-well potential.

The exposition and examples considered deal with conservative systems relaxing toward an equilibrium steady state. The considered inequalities hold in nonconservative systems relaxing toward a nonequilibrium steady state once the potential is replaced by the pseudopotential defined by the stationary density, in which case they bound the excess entropy production rate.

II. PHYSICAL FLOW AND OPTIMAL TRANSPORT

A. Fokker-Planck equation

Consider an overdamped Brownian particle at position $\boldsymbol{x}$ in n-dimensional space, being in contact with a heat bath at temperature T and subject to a potential $\psi \equiv \psi(\boldsymbol{x})$. Its stochastic dynamics is described by the equilibrium Langevin equation [3],

$$d\boldsymbol{x} = -\nabla\psi\, dt + \sqrt{2T}\, d\boldsymbol{W}, \tag{1}$$

where $d\boldsymbol{W}$ are standard vector Brownian motion increments [39], and the mobility and Boltzmann constant are set to unity and not considered. The corresponding probability density $p \equiv p(\boldsymbol{x}, t)$ evolves according to the Fokker-Planck equation [16–18],

$$\partial_t p = \nabla \cdot [p \nabla(\psi + T \ln p)], \tag{2}$$

where $-\nabla(\psi + T \ln p)$ is the local mean velocity. Assume the potential ψ to be such that a unique invariant density exists defined by $\partial_t p|_{p^*} = 0$. The latter is then given by the Gibbs-Boltzmann distribution

$$p^* = \frac{1}{Z} \exp\left(-\frac{\psi}{T}\right), \tag{3}$$

*Contact author: andrea.auconi@gmail.com

Published by the American Physical Society under the terms of the Creative Commons Attribution 4.0 International license. Further distribution of this work must maintain attribution to the author(s) and the published article's title, journal citation, and DOI.

where $Z \equiv \int d\boldsymbol{x}\, \exp(-\psi/T)$ ensures normalization. Quantities evaluated at the steady state are marked with an asterisk $(*)$. In terms of the steady-state density, one can rewrite $\boldsymbol{\nabla}(\psi + T \ln p) = T\boldsymbol{\nabla} \ln(p/p^*)$.

B. Free energy dynamics

The Helmholtz free energy [3] is defined as

$$\mathcal{F} \equiv U - TS, \tag{4}$$

where $U[p] \equiv \int d\boldsymbol{x}\, p\psi$ is the potential energy and $S[p] \equiv -\int d\boldsymbol{x}\, p \ln p$ is Shannon entropy. The equilibrium free energy reads $\mathcal{F}^* = -T \ln Z$.

The relative entropy [40] of a distribution $p \equiv p(\boldsymbol{x})$ from a reference distribution $q \equiv q(\boldsymbol{x})$ is defined as $D[p\|q] \equiv \int d\boldsymbol{x}\, p \ln(p/q) \geqslant 0$, and it is nonnegative by Jensen's inequality. The relative entropy from the invariant density is related to the free energy [20–24] as

$$D \equiv D[p\|p^*] = \frac{1}{T}(\mathcal{F} - \mathcal{F}^*) \geqslant 0. \tag{5}$$

Since $\mathcal{F}^*$ is constant, the dynamics of the relative entropy is proportional to that of the free energy, $T d_t D = d_t \mathcal{F}$, which yields

$$d_t D = -T \int d\boldsymbol{x}\, p \left\| \boldsymbol{\nabla} \ln\left(\frac{p}{p^*}\right)\right\|^2 \leqslant 0, \tag{6}$$

whose negativity guarantees the Glansdorff-Prigogine stability of the steady state [41–43]. This relation of Eq. (6) between a relative Fisher information and the time derivative of a relative entropy is a type of De Bruijn's identity [44]. The quantity $-d_t D$ is also known as the Hatano-Sasa excess entropy production rate [20–24]. Note that the restriction to a purely conservative dynamics Eq. (1) does not explicitly impact $d_t D$, as indeed nonconservative forces only enter at the second time derivative $d_t^2 D$; see Refs. [45,46].

C. Optimal transport

The Wasserstein distance $\mathcal{W}$ quantifies the minimum quadratic cost of transforming one probability distribution into another [19],

$$\mathcal{W}^2(p, q) \equiv \inf_{\pi \in \Pi(p,q)} \int d\boldsymbol{x} d\boldsymbol{y}\, \pi(\boldsymbol{x}, \boldsymbol{y}) \|\boldsymbol{x} - \boldsymbol{y}\|^2, \tag{7}$$

where $\Pi(p, q)$ is the set of all joint probability distributions $\pi(\boldsymbol{x}, \boldsymbol{y})$ whose marginals are the given densities $\int d\boldsymbol{y}\, \pi = p(\boldsymbol{x})$ and $\int d\boldsymbol{x}\, \pi = q(\boldsymbol{y})$.

This optimal transport problem admits an equivalent formulation, due to Benamou and Brenier [27], as the minimization of the time-integrated kinetic energy of a fluid having the given densities as temporal boundary conditions. Such optimal fluid dynamics, reviewed in the Supplemental Material (SM) [47], is written in terms of the time-dependent velocity field $\boldsymbol{\nabla}\lambda_\tau \equiv \boldsymbol{\nabla}\lambda_\tau(\boldsymbol{x})$ as

$$\begin{aligned} \partial_\tau p_\tau &= -\boldsymbol{\nabla} \cdot (p_\tau \boldsymbol{\nabla}\lambda_\tau), \\ \partial_\tau \lambda_\tau &= -\tfrac{1}{2} \|\boldsymbol{\nabla}\lambda_\tau\|^2, \end{aligned} \tag{8}$$

where τ is a fictitious time variable which parametrizes the optimal transport path p_τ in $\tau \in [0, 1]$. As seen from the total derivative $d_\tau \boldsymbol{\nabla}\lambda_\tau(\boldsymbol{x}_\tau) = \boldsymbol{0}$ along the trajectory $\boldsymbol{x}_\tau$ defined by $d_\tau \boldsymbol{x}_\tau = \boldsymbol{\nabla}\lambda_\tau(\boldsymbol{x}_\tau)$, Eq. (8) describes fluid particles traveling on straight lines at constant velocity. Accordingly, the Wasserstein distance can be evaluated from the field λ_τ at any transport time point as $\mathcal{W}^2(p_0, p_1) = \int d\boldsymbol{x}\, p_\tau \|\boldsymbol{\nabla}\lambda_\tau\|^2$, and the optimal map $\boldsymbol{T}$ that transforms the initial distribution p to the final target q is written $\boldsymbol{T}(\boldsymbol{x}) = \boldsymbol{x} + \boldsymbol{\nabla}\lambda_0(\boldsymbol{x})$.

Finding the particular initial field configuration $\lambda_0(\boldsymbol{x})$ that solves this boundary value problem is approached with numerical techniques like the entropically regularized optimal transport via the Sinkhorn-Knopp algorithm [48]. See Fig. 1 for an illustration of the optimal transport in comparison to gradient descent and to the physical flow defined by the local mean velocity.

III. THERMODYNAMIC BOUNDS IN THE OTTO–VILLANI FRAMEWORK

A. The general bound

Consider the optimal transport from the current density p at physical time t to the steady-state density p^*. Let us introduce the notation $f_\tau \equiv f(\boldsymbol{x}, t, \tau)$ for any spatial field which depends on the transport time τ and use the convention $f \equiv f_0$ for the initial transport time $\tau = 0$. Similarly, for the relative entropy functional, we define $D_\tau \equiv D[p_\tau\|p^*]$ and $D \equiv D[p\|p^*]$. Note that for any particular configuration of the physical density p at any time t, there exists an optimal transport dynamics p_τ described by $\lambda_\tau \equiv \lambda(\boldsymbol{x}, t, \tau)$ through Eq. (8) with $\tau \in [0, 1]$ having the steady-state density $p_1 = p^*$ as the target. We denote the corresponding Wasserstein distance as $\mathcal{W} \equiv \mathcal{W}(p, p^*)$. The notation adopted in this section reflects that we consider t as a fixed parameter here and study the corresponding optimal transport as a function of τ.

Under the optimal transport dynamics, described by Eq. (8), the relative entropy evolves as

$$d_\tau D_\tau = \int d\boldsymbol{x}\, p_\tau\, \boldsymbol{\nabla}\lambda_\tau \cdot \boldsymbol{\nabla} \ln\left(\frac{p_\tau}{p^*}\right). \tag{9}$$

By applying the Cauchy-Schwarz inequality at $\tau = 0$ and recognizing the definition Eq. (6), one obtains the thermodynamic bound

$$\sqrt{-d_t D} \geqslant \frac{\sqrt{T}}{\mathcal{W}} |(d_\tau D_\tau)_{\tau=0}| \geqslant 0, \tag{10}$$

which is the fundamental connection between optimal transport and physical relaxation as derived by Otto and Villani [35,49]. Its nonnegativity establishes it as a refinement of the second law of thermodynamics. The equality case is obtained when physical local mean velocity $-T\boldsymbol{\nabla} \ln(p/p^*)$ and optimal transport velocity $\boldsymbol{\nabla}\lambda$ are globally proportional. Recall that the notation $(d_\tau D_\tau)_{\tau=0}$ here means the time derivative along the optimal transport path defined by p and p^*, evaluated at the initial transport time $\tau = 0$ where the physical and optimal transport densities coincide, $p_0 = p$. This implicitly means to consider the initial fluid velocity field $\boldsymbol{\nabla}\lambda = \boldsymbol{\nabla}\lambda(\boldsymbol{x}, t, 0)$ solution of the optimal transport problem at physical time t.

This inequality provides a geometric perspective on the slowing down of relaxation in the presence of potential barriers, which is at the basis of the Markovian Mpemba effect

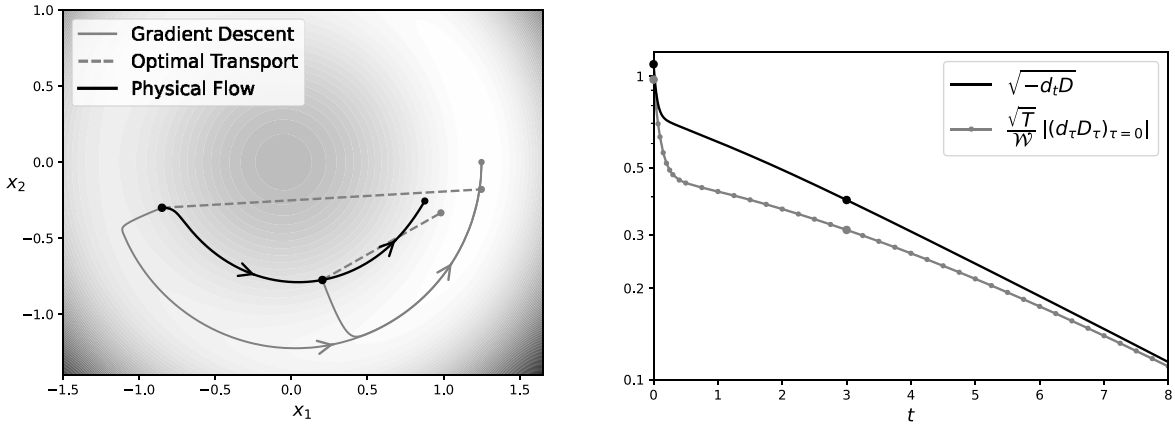


FIG. 1. Left panel: The gradient descent velocity is $-\nabla\psi$, based only on the potential. The physical flow is defined as the local mean velocity $-\nabla(\psi + T\ln p)$, which also accounts for the temperature-driven diffusion. The corresponding optimal transport ensemble p_τ is made of fluid particles of constant velocity $\nabla\lambda_\tau(\boldsymbol{x}_\tau)$. Consider a tilted Mexican hat potential, $\psi(\boldsymbol{x}) = \boldsymbol{z}\cdot\boldsymbol{x} - \alpha\|\boldsymbol{x}\|^2 + \beta\|\boldsymbol{x}\|^4$, with $\alpha = 3$, $\beta = 1$, $T = 0.3$, and $\boldsymbol{z} = 0.3\hat{\boldsymbol{x}}_1$ along the x_1 axis, and an ensemble brought out of equilibrium at $t = 0$ by switching the bias as $\boldsymbol{z} \to -\boldsymbol{z}$. Numerical integration of the physical flow shows how trajectories typically bend in the presence of a potential barrier along the geodesic. Gradient descent and optimal transport are shown from two points along the same physical trajectory, as at each time t the current density $p(t)$ defines its own optimal transport path toward p^*. Right panel: We compare the instantaneous relaxation speed $\sqrt{-d_tD}$ (black line) to the lower bound of Eq. (10) (gray line). The bound is least tight shortly after the switch and local relaxation, when the physical flow is redirected along the valley around the central peak. It approaches saturation at later times, when a single slow relaxation mode dominates and the density is close to the steady state $p \simeq p^*$. Neither the HWI [Eq. (14)] nor the LSI [Eq. (15)] provides a positive bound here.

[11–15]. Consider a landscape where two or more wells are separated by large potential barriers. If a density is released within one of these wells, it first undergoes a rapid relaxation of timescale t_{fast} until it locally reproduces the invariant shape, $p(t_{\text{fast}}) \approx \mathbb{I}_{x\in\Omega}\, p^*/\int_\Omega d\boldsymbol{x}\, p^*$, where Ω denotes the corresponding region. Then, for $t > t_{\text{fast}}$, a kinetic bottleneck is predicted, since both d_tD and $(d_\tau D_\tau)_{\tau=0}$ integrate the factor $p\nabla\ln(p/p^*) \approx \boldsymbol{0}$, which is small in the wells as $\nabla\ln(p/p^*)|_{x\in\Omega} \approx \boldsymbol{0}$ and small on the peaks as $p|_{x\notin\Omega} \approx 0$ for large barriers. Crucially, in $n \geqslant 2$ dimensions the physical dynamics may exploit alternative pathways around the barriers rather than following the direct optimal transport path, see Fig. 1, rendering Eq. (10) a strict inequality. Note that even in one dimension, where no alternative pathways exist, Eq. (10) is typically strict as the physical flow and the geodesic, in general, point in different directions in the space of densities.

In other words, the right-hand side of Eq. (10) is the relaxation speed that the ensemble would have if its local mean velocity were replaced by its projection onto the geodesic. This constrained speed is set by the slope of the free energy along the geodesic, $T(d_\tau D_\tau)_{\tau=0}$, which is offset by the energetic term $\int d\boldsymbol{x}\, p\,\nabla\lambda\cdot\nabla\psi$ when the direct route has to climb a potential barrier. The physical flow instead deviates from the geodesic, for example, around the barriers, and thereby relaxes faster than along the unfavorable direct route.

Let us note that, being a lower bound, Eq. (10) cannot by itself imply a slowing down of relaxation. In fact, its gap quantifies the speedup of the physical flow with respect to the direct transport route, while a small lower bound implies a slow relaxation only close to saturation.

B. HWI inequality

For any smooth function $f(s)$, the Taylor identity $f(1) = f(0) + f'(0) + \int_0^1 ds\,(1-s)f''(s)$ holds, which applied to D_τ with respect to the optimal transport time τ reads

$$-(d_\tau D_\tau)_{\tau=0} = D + \int_0^1 d\tau\,(1-\tau)d_\tau^2 D_\tau, \tag{11}$$

where we used $D_1 = D[p^*\|p^*] = 0$, and the second derivative is computed as

$$d_\tau^2 D_\tau = \int d\boldsymbol{x}\, p_\tau(\nabla\lambda_\tau\cdot\nabla\nabla\psi\cdot\nabla\lambda_\tau/T + \|\nabla\nabla\lambda_\tau\|^2), \tag{12}$$

where $\|\nabla\nabla\lambda_\tau\|^2$ denotes the Frobenius norm.

The minimum convexity of the potential ψ is defined via the Loewner order as

$$\kappa \equiv \inf_{\boldsymbol{x}}\min_{\boldsymbol{u}}\frac{\boldsymbol{u}\cdot\nabla\nabla\psi\cdot\boldsymbol{u}}{\|\boldsymbol{u}\|^2}, \tag{13}$$

which means that the eigenvalues of its Hessian matrix $\nabla\nabla\psi$ are bounded below by κ across the domain. From this global majorization [Eq. (13)] and the nonnegativity $\|\nabla\nabla\lambda_\tau\|^2 \geqslant 0$, the second derivative [Eq. (12)] is bounded by $d_\tau^2 D_\tau \geqslant (\kappa/T)\mathcal{W}^2$ for all transport times $0 \leqslant \tau \leqslant 1$. Substituting into Eq. (11) and using the inequality Eq. (10) yields

$$\sqrt{-d_tD} \geqslant \frac{\sqrt{T}}{\mathcal{W}}D + \frac{\mathcal{W}}{\sqrt{T}}\frac{\kappa}{2}, \tag{14}$$

which is the celebrated HWI inequality [35]. It depends on the optimal transport problem only through the Wasserstein distance $\mathcal{W}$, and it unifies other functional inequalities also based on the minimum convexity κ, like the LSI and Talagrand inequality. The equality case in the HWI is obtained if the potential has constant convexity $\nabla\nabla\psi = \kappa\boldsymbol{I}$ (meaning p^* is a Gaussian), and p is a pure translation of p^*. Note that, while Eq. (14) holds for nonconvex potentials with $\kappa < 0$, the right-hand side is positive only for $\kappa > -2TD/\mathcal{W}^2$, therefore

the HWI inequality is not a general refinement of the second law of thermodynamics.

Let us discuss the three majorization steps taken to obtain the HWI inequality from the intermediate bound Eq. (10). First, the absolute value majorization $|(d_\tau D_\tau)_{\tau=0}| \geqslant -(d_\tau D_\tau)_{\tau=0}$ restricts the usefulness to regimes where the relative entropy decreases along the geodesic at $\tau = 0$. Then, the minimum convexity majorization $\boldsymbol{\nabla}\lambda_\tau \cdot \boldsymbol{\nabla}\boldsymbol{\nabla}\psi \cdot \boldsymbol{\nabla}\lambda_\tau \geqslant \kappa \|\boldsymbol{\nabla}\lambda_\tau\|^2$ effectively compares the state to the worst-case scenario of having to cross the sharpest peak in the landscape. Finally, the Frobenius norm majorization neglects the entropic impact of expansions and contractions, as $\boldsymbol{\nabla}\boldsymbol{\nabla}\lambda_\tau$ is the spatial gradient of the optimal transport velocity field $\boldsymbol{\nabla}\lambda_\tau$. Note that dimensional refinements to this term have been obtained [50] by the trace inequality $\|\boldsymbol{\nabla}\boldsymbol{\nabla}\lambda_\tau\|^2 \geqslant (\nabla^2\lambda_\tau)^2/n$; see also the SM [47].

C. Logarithmic Sobolev inequality

One may be interested in a thermodynamic bound independent of the optimal transport problem. This is the case of the LSI, which could be derived either directly from the physical dynamics as reviewed in the SM [47] or as a consequence of the HWI inequality as done in [35]. Indeed, by taking the minimum of the right-hand side of Eq. (14) with respect to the Wasserstein distance $\mathcal{W}$ as if it were a free parameter, it yields the LSI

$$-d_t D \geqslant 2\kappa D. \tag{15}$$

Clearly this inequality becomes trivial if $\kappa < 0$, meaning when the potential is not convex everywhere. When $\kappa > 0$, the LSI guarantees the exponential convergence to the steady state as $D[p(t)\|p^*] \leqslant D[p(0)\|p^*]\exp(-2\kappa t)$.

D. Nonequilibrium steady states

While the derivations above consider conservative dynamics relaxing to an equilibrium Gibbs-Boltzmann distribution, the geometric framework naturally extends to systems driven by nonconservative forces. Let us first note that, in a nonequilibrium steady state, the presence of persistent probability currents does not explicitly impact the instantaneous relaxation speed measured by $d_t D$, see, e.g., Refs. [45,46]. We also note that the optimal transport map depends solely on the spatial boundary densities p and p^*, independently of the underlying physical fluxes. Consequently, the intermediate bound of Eq. (10) applies equally to relaxation toward an equilibrium or a nonequilibrium steady state. The subsequent HWI and LSI inequalities [Eqs. (14) and (15)] also remain formally valid for nonequilibrium systems, with the required modification that the minimum convexity should be evaluated on the pseudopotential $\psi_{\text{eff}} \equiv -T \ln p^*$ defined by the steady-state density.

IV. NUMERICAL ILLUSTRATIONS

A. Illustration in a double-well potential

Consider the Landau-Ginzburg double-well potential in 1D, $\psi(x, t \geqslant 0) = -\alpha x^2 + \beta x^4$, with $\alpha > 0$ and $\beta > 0$. The ensemble is initially in thermal equilibrium with respect to a tilted version of the potential, $\psi(x, t < 0) = \psi(x, t \geqslant 0) + \gamma x$, where the bias $\gamma < 0$ forces the probability mass into the right well. At time $t = 0$, the bias is removed and the system relaxes toward the symmetric bimodal equilibrium distribution $p^* \sim \exp(-\psi(x, t \geqslant 0)/T)$. This transition from a localized state to a symmetric delocalized state across an energy barrier is analogous to the reverse process of bit erasure [7–10]. Note that the one-dimensional scenario is uniquely tractable as the optimal transport map can be constructed through the monotonic matching of cumulative distributions [51]. If F and F^* are smooth and strictly increasing cumulative distributions, the optimal transport map from F to F^* is given by the composition $(F^*)^{-1} \circ F$. As demonstrated in Fig. 2, the fundamental bound Eq. (10) becomes tight only in the long-time limit. At early times $t < t_{\text{fast}} = 1/(4\alpha)$ the physical flow and optimal transport fields are not globally proportional due to the simultaneous presence of fast intrawell and slow interwell relaxation. Once the intrawell dynamics reaches a metastable local equilibrium, the only surviving process is the slow leakage of mass across the central energy barrier. In this latter single-mode regime, the gap persists because the physical current $-pT\,\partial_x \ln(p/p^*)$ becomes roughly symmetric about the barrier top, draining one well while filling the other, whereas the optimal transport flux $p\partial_x\lambda$ is drawn mainly from the overpopulated well. Finally, in the vicinity of

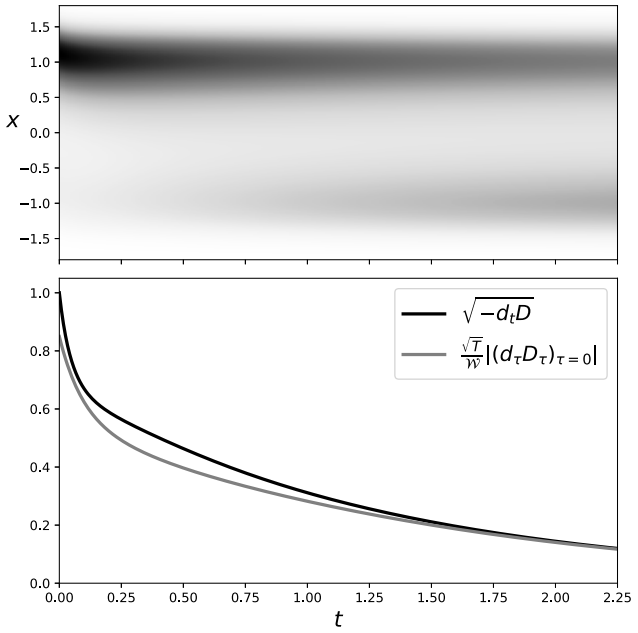


FIG. 2. Thermal decay of a stored bit (reverse of bit erasure) in a Landau-Ginzburg double-well potential $\psi = -\alpha x^2 + \beta x^4$. The parameters are set to $T = 1$, $\alpha = 2$, $\beta = 1$, with an initial confining bias $\gamma = -1$. Top: Relaxation of the probability density $p(x, t)$ over the central energy barrier toward a symmetric bimodal steady state. Bottom: The instantaneous relaxation speed $\sqrt{-d_t D}$ (black line) compared to the lower bound of Eq. (10) (gray line) based on optimal transport. Note the acceleration change around the local intrawell relaxation timescale $t_{\text{fast}} = 1/(4\alpha)$, after which the dynamics is dominated by the slow interwell relaxation. The HWI Eq. (14) does not provide a positive bound here as in the considered time interval it holds uniformly $\kappa < -2TD/\mathcal{W}^2$.

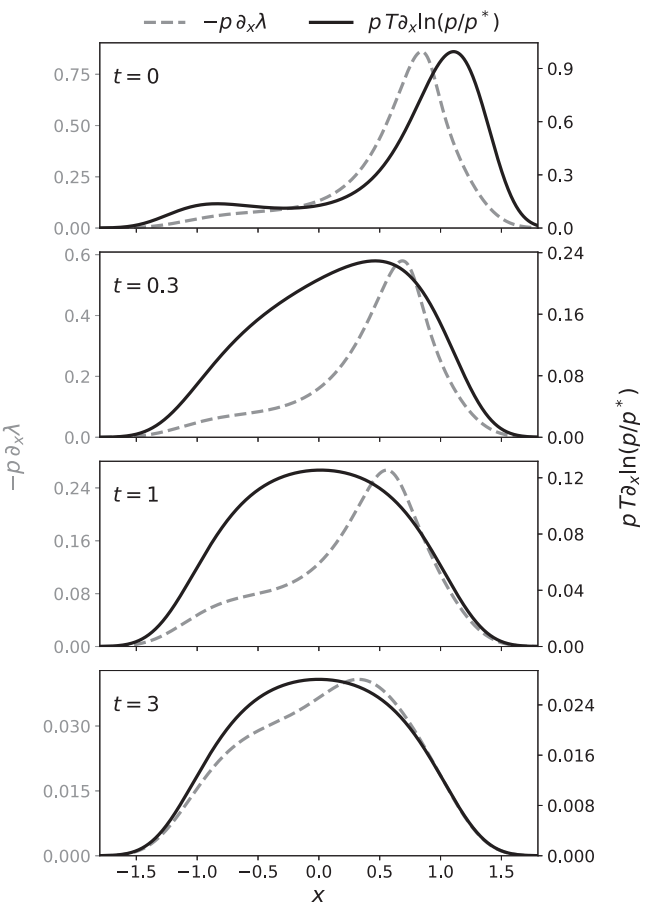


FIG. 3. Probability currents during the relaxation of Fig. 2. The optimal transport flux $p\,\partial_x\lambda$ (gray dashed line) and the physical current $-pT\,\partial_x \ln(p/p^*)$ (black line), both with inverted sign and on separate vertical scales, so proportional currents overlap.

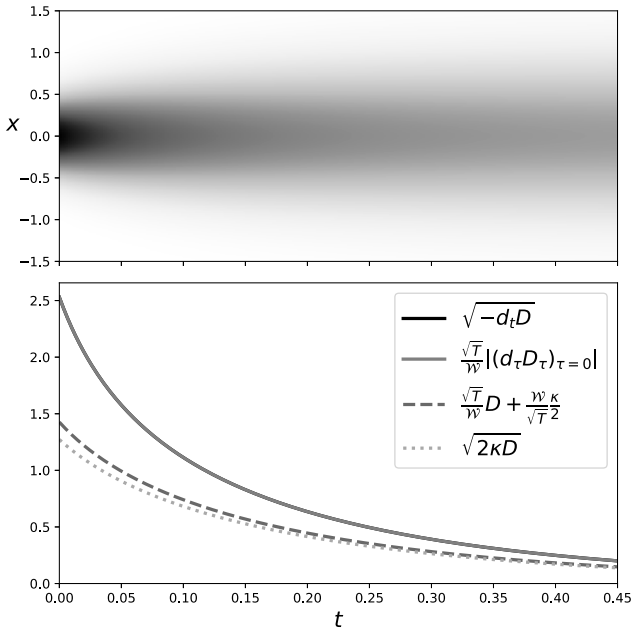


FIG. 4. Thermal expansion in a harmonic potential. The parameters are set to $T = 1$, $\kappa = 2$, and initial stiffness $\gamma = 10$. Top: Symmetric expansion of the Gaussian probability density $p(x, t)$ toward the broader steady state. Bottom: The lower bound of Eq. (10) (gray line) saturates at all times the instantaneous relaxation speed $\sqrt{-d_t D}$ (black line, hidden under the gray line). Here the bounds from the HWI [Eq. (14)] (gray dashed line) and LSI [Eq. (15)] (gray dotted line) are nontrivial.

the steady state $p \simeq p^*$, the physical flow and optimal transport fields become globally proportional therefore saturating the bound; see also Fig. 3 for a spatial comparison of the physical and optimal transport flows.

B. Saturation in a Gaussian expansion

Consider a thermal expansion in a harmonic potential, $\psi(x, t \geqslant 0) = \frac{1}{2}\kappa x^2$. The system is initially prepared in thermal equilibrium inside a more confining potential $\psi(x, t < 0) = \frac{1}{2}\gamma x^2$ with $\gamma > \kappa$. At time $t = 0$, the trap is instantaneously changed $\gamma \to \kappa$ and the ensemble expands symmetrically toward a broader Gaussian steady state. The probability density $p(x, t)$ remains perfectly Gaussian at all times during the relaxation process, and the optimal transport map is linear. This case can be treated analytically, see the SM [47]. As shown in Fig. 4, while the fundamental bound Eq. (10) is saturated, because the expansion changes the entropy of the system it holds strictly $\|\partial_x^2 \lambda_\tau\|^2 > 0$, therefore the HWI inequality Eq. (14) is not saturated. The LSI Eq. (15) is looser than HWI as the corresponding Talagrand inequality $D \geqslant \kappa \mathcal{W}^2/(2T)$ saturates only for pure translations.

The reverse quench $\kappa \to \gamma$, which compresses the density along the same geodesic, is also Gaussian and saturates Eq. (10). For a harmonic potential, the HWI fully includes the energetic curvature in Eq. (12) and neglects only the entropic term, which enters as an integrand $p_\tau(1-\tau)\|\partial_x^2 \lambda_\tau\|^2$ in Eq. (11). At the quench, the two processes traverse the same geodesic in opposite directions, so this weighted integral is larger for the expansion, which starts at the narrower density where $\|\partial_x^2 \lambda_\tau\|^2$ is largest. Moreover, the exact slope $-(d_\tau D_\tau)_{\tau=0} = \int_0^1 d\tau\, d_\tau^2 D_\tau$, which follows from $(d_\tau D_\tau)_{\tau=1} = 0$, contains the unweighted integrand $p_\tau \|\partial_x^2 \lambda_\tau\|^2$ which gives the same integral for both directions, plus an energetic term proportional to the final stiffness which is smaller for the expansion. The relative gap of the HWI is therefore larger for the expansion at the quench, and the SM [47] shows that this ordering holds at all times t.

V. DISCUSSION

In conclusion, functional inequalities in the Otto-Villani HWI framework provide a geometric perspective on the instantaneous relaxation speed of continuous systems. While the classical HWI inequality reduces the impact of the potential landscape to its global minimum convexity, the intermediate bound captures local details of the free energy landscape through a projection of the physical flow onto the optimal transport geodesic, and its tightness typically stays finite also in non-convex potentials.

While the Benamou–Brenier formulation of optimal transport has been fruitfully employed in the stochastic thermodynamics literature to derive thermodynamic speed limits, the

Otto–Villani HWI framework appears to have remained unexplored in this context. Its lower bounds on the dissipation rate are expressed in terms of the instantaneous density and the steady-state density, and are thus complementary to existing thermodynamic speed limits [26,28–31] which are expressed in terms of the density at two different times along the process. In particular, in the absence of nonconservative forces, such speed limits either vanish or they reduce to the definition of the entropy production rate as the two times approach each other, see the SM [47], whereas Eq. (10) is a nontrivial bound on the instantaneous relaxation speed, obtained by comparing the direction of the physical flow with the geodesic toward the steady state.

Finally, we note that the general bound Eq. (10) is not meant here as a computational shortcut, since the relaxation speed is directly accessible from the instantaneous density if the steady state is known, while the bound requires solving an optimal transport problem. Its value is rather in the geometric intuition it offers, as it measures how far the physical relaxation deviates from the direct transport route toward the steady state, and it identifies the majorization steps that make the HWI and LSI inequalities loose in nonconvex landscapes.

ACKNOWLEDGMENT

I thank S. Ito for fruitful discussions.

DATA AVAILABILITY

There are no publicly available research data or software supporting this manuscript. Requests for further information or data should be sent to the author.

[1] R. Kubo, M. Toda, and N. Hashitsume, *Statistical Physics II: Nonequilibrium Statistical Mechanics*, Springer Series in Solid-State Sciences Vol. 31 (Springer Science & Business Media, Berlin, 2012).

[2] P. Gaspard, *The Statistical Mechanics of Irreversible Phenomena* (Cambridge University Press, Cambridge, 2022).

[3] U. Seifert, Stochastic thermodynamics, fluctuation theorems and molecular machines, Rep. Prog. Phys. **75**, 126001 (2012).

[4] G. Lan, P. Sartori, S. Neumann, V. Sourjik, and Y. Tu, The energy–speed–accuracy trade-off in sensory adaptation, Nat. Phys. **8**, 422 (2012).

[5] S. Ito and T. Sagawa, Maxwell's demon in biochemical signal transduction with feedback loop, Nat. Commun. **6**, 7498 (2015).

[6] C. J. Edelson, S. Setayeshgar, W. Bialek, and R. R. de Ruyter van Steveninck, Context dependent adaptation in a neural computation, arXiv:2509.01760.

[7] A. Bérut, A. Arakelyan, A. Petrosyan, S. Ciliberto, R. Dillenschneider, and E. Lutz, Experimental verification of Landauer's principle linking information and thermodynamics, Nature (London) **483**, 187 (2012).

[8] K. Proesmans, J. Ehrich, and J. Bechhoefer, Finite-time Landauer principle, Phys. Rev. Lett. **125**, 100602 (2020).

[9] J. S. Lee, S. Lee, H. Kwon, and H. Park, Speed limit for a highly irreversible process and tight finite-time Landauer's bound, Phys. Rev. Lett. **129**, 120603 (2022).

[10] S. Oikawa, Y. Nakayama, S. Ito, T. Sagawa, and S. Toyabe, Experimentally achieving minimal dissipation via thermodynamically optimal transport, Nat. Commun. **16**, 10424 (2025).

[11] Z. Lu and O. Raz, Nonequilibrium thermodynamics of the Markovian Mpemba effect and its inverse, Proc. Natl. Acad. Sci. USA **114**, 5083 (2017).

[12] G. Teza, J. Bechhoefer, A. Lasanta, O. Raz, and M. Vucelja, Speedups in nonequilibrium thermal relaxation: Mpemba and related effects, Phys. Rep. **1164**, 1 (2026).

[13] A. Lapolla and A. Godec, Faster uphill relaxation in thermodynamically equidistant temperature quenches, Phys. Rev. Lett. **125**, 110602 (2020).

[14] J. Meibohm, D. Forastiere, T. Adeleke-Larodo, and K. Proesmans, Relaxation-speed crossover in anharmonic potentials, Phys. Rev. E **104**, L032105 (2021).

[15] M. Ibáñez, C. Dieball, A. Lasanta, A. Godec, and R. A. Rica, Heating and cooling are fundamentally asymmetric and evolve along distinct pathways, Nat. Phys. **20**, 135 (2024).

[16] H. Risken, Fokker-Planck equation, in *The Fokker-Planck Equation: Methods of Solution and Applications* (Springer, Berlin, 1989), pp. 63–95.

[17] R. Jordan, D. Kinderlehrer, and F. Otto, The variational formulation of the Fokker–Planck equation, SIAM J. Math. Anal. **29**, 1 (1998).

[18] S. Ito, Geometric thermodynamics for the Fokker–Planck equation: Stochastic thermodynamic links between information geometry and optimal transport, Inf. Geom. **7**, 441 (2024).

[19] C. Villani, *Optimal Transport: Old and New*, Grundlehren der mathematischen Wissenschaften Vol. 338 (Springer, Berlin, 2009).

[20] T. Hatano and S.-I. Sasa, Steady-state thermodynamics of Langevin systems, Phys. Rev. Lett. **86**, 3463 (2001).

[21] C. Van den Broeck and M. Esposito, Three faces of the second law. II. Fokker-Planck formulation, Phys. Rev. E **82**, 011144 (2010).

[22] M. Esposito and C. Van den Broeck, Second law and Landauer principle far from equilibrium, Europhys. Lett. **95**, 40004 (2011).

[23] A. Dechant, S.-I. Sasa, and S. Ito, Geometric decomposition of entropy production in out-of-equilibrium systems, Phys. Rev. Res. **4**, L012034 (2022).

[24] A. Kolchinsky, A. Dechant, K. Yoshimura, and S. Ito, Generalized free energy and excess/housekeeping decomposition in nonequilibrium systems: From large deviations to thermodynamic speed limits, Phys. Rev. Res. **8**, 023025 (2026).

[25] N. Shiraishi, K. Funo, and K. Saito, Speed limit for classical stochastic processes, Phys. Rev. Lett. **121**, 070601 (2018).

[26] N. Shiraishi and K. Saito, Information-theoretical bound of the irreversibility in thermal relaxation processes, Phys. Rev. Lett. **123**, 110603 (2019).

[27] J.-D. Benamou and Y. Brenier, A computational fluid mechanics solution to the Monge-Kantorovich mass transfer problem, Numer. Math. **84**, 375 (2000).

[28] E. Aurell, K. Gawędzki, C. Mejía-Monasterio, R. Mohayaee, and P. Muratore-Ginanneschi, Refined second law of thermo-

dynamics for fast random processes, J. Stat. Phys. **147**, 487 (2012).
[29] A. Dechant and Y. Sakurai, Thermodynamic interpretation of Wasserstein distance, arXiv:1912.08405.
[30] M. Nakazato and S. Ito, Geometrical aspects of entropy production in stochastic thermodynamics based on Wasserstein distance, Phys. Rev. Res. **3**, 043093 (2021).
[31] T. Van Vu and K. Saito, Thermodynamic unification of optimal transport: Thermodynamic uncertainty relation, minimum dissipation, and thermodynamic speed limits, Phys. Rev. X **13**, 011013 (2023).
[32] R. Sabbagh, O. Movilla Miangolarra, and T. T. Georgiou, Wasserstein speed limits for Langevin systems, Phys. Rev. Res. **6**, 033308 (2024).
[33] N. Shiraishi, Wasserstein distance in speed limit inequalities for Markov jump processes, J. Stat. Mech. (2024) 074003.
[34] A. Zhong and M. R. DeWeese, Beyond linear response: Equivalence between thermodynamic geometry and optimal transport, Phys. Rev. Lett. **133**, 057102 (2024).
[35] F. Otto and C. Villani, Generalization of an inequality by Talagrand and links with the logarithmic Sobolev inequality, J. Funct. Anal. **173**, 361 (2000).
[36] J. Lott and C. Villani, Ricci curvature for metric-measure spaces via optimal transport, Ann. Math. **169**, 903 (2009).
[37] I. Gentil, C. Léonard, L. Ripani, and L. Tamanini, An entropic interpolation proof of the HWI inequality, Stoch. Process. Appl. **130**, 907 (2020).
[38] I. Karatzas, W. Schachermayer, and B. Tschiderer, A trajectorial approach to the gradient flow properties of Langevin–Smoluchowski diffusions, Theory Probab. Its Appl. **66**, 668 (2022).
[39] I. Karatzas and S. Shreve, *Brownian Motion and Stochastic Calculus* (Springer, New York, 2014).
[40] S.-I. Amari, *Information Geometry and Its Applications* (Springer, Tokyo, 2016).
[41] P. Glansdorff, G. Nicolis, and I. Prigogine, The thermodynamic stability theory of non-equilibrium states, Proc. Natl. Acad. Sci. USA **71**, 197 (1974).
[42] S. Ito, Information geometry, trade-off relations, and generalized Glansdorff–Prigogine criterion for stability, J. Phys. A: Math. Theor. **55**, 054001 (2022).
[43] C. Maes and K. Netočný, Revisiting the Glansdorff–Prigogine criterion for stability within irreversible thermodynamics, J. Stat. Phys. **159**, 1286 (2015).
[44] A. Dembo, T. M. Cover, and J. A. Thomas, Information theoretic inequalities, IEEE Trans. Inf. Theory **37**, 1501 (1991).
[45] A. Auconi, Nonequilibrium relaxation inequality on short timescales, Phys. Rev. Lett. **134**, 087104 (2025).
[46] A. Auconi and S. Ito, Information-geometric signatures of nonconservative driving, arXiv:2605.03757.
[47] See Supplemental Material at http://link.aps.org/supplemental/10.1103/6zkl-1vnk for a brief review of optimal transport theory and the free energy dynamics in the Fokker-Planck equation. This includes Refs. [52–56].
[48] G. Peyré and M. Cuturi, *Computational Optimal Transport: With Applications to Data Science* (Now Foundations and Trends, Hanover, MA, 2019).
[49] This exact form is not explicitly written in the original Ref. [35], but it is an immediate intermediate bound within the HWI inequality derivation therein.
[50] M. Erbar, K. Kuwada, and K.-T. Sturm, On the equivalence of the entropic curvature-dimension condition and Bochner's inequality on metric measure spaces, Invent. math. **201**, 993 (2015).
[51] O. Rioul, Optimal transportation to the entropy-power inequality, in *Proceedings of the 2017 Information Theory and Applications Workshop (ITA)* (IEEE, Piscataway, NJ, 2017), pp. 1–5.
[52] C. Villani, *Topics in Optimal Transportation*, Graduate Studies in Mathematics Vol. 58 (American Mathematical Society, Providence, RI, 2021).
[53] A. Dechant and S.-I. Sasa, Entropic bounds on currents in Langevin systems, Phys. Rev. E **97**, 062101 (2018).
[54] S. Ito and A. Dechant, Stochastic time evolution, information geometry, and the Cramér-Rao bound, Phys. Rev. X **10**, 021056 (2020).
[55] I. Ekeland and R. Temam, *Convex Analysis and Variational Problems* (SIAM, Philadelphia, 1999).
[56] R. Bao, C. Du, Z. Cao, and Z. Hou, Universal trade-off between irreversibility and intrinsic timescale in thermal relaxation with applications to thermodynamic inference, Phys. Rev. E **112**, 044134 (2025).